



Research Article

Potential implementation of the woody biochar waste as an eco-friendly soil stabilization material in sandy environments

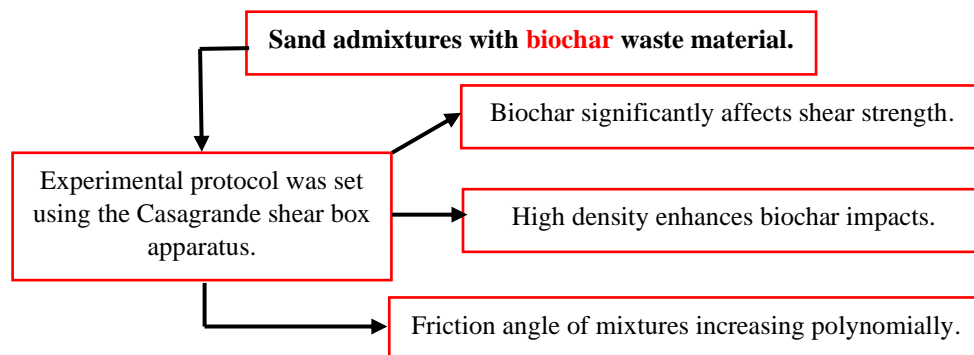
Mohammed Megrouse¹, Youcef Mahmoudi^{1*}, Abdellah Cherif Taiba^{1,2*}, Hamou Azaiez¹, Mostefa Belkhatir^{1,3}

- 1 Laboratory of Material Sciences and Environment, Hassiba Ben Bouali, University of Chlef, Chlef (Algeria)
 - 2 Laboratory of Architecture, Cities and Environment, Hassiba Ben Bouali, University of Chlef, Chlef (Algeria)
 - 3 Alexander von Humboldt Foundation Researcher, Berlin (Germany)
- *Correspondence : y.mahmoudi@univ-chlef.dz (Y. Mahmoudi)

Received: 14.05.24; **Accepted:** 25.09.24; **Published:** 12.12.24

Citation: Megrouse, M., Mahmoudi, Y., Cherif Taiba, A., Azaiez, H., and Belkhatir, M. (2024). Potential implementation of the woody biochar waste as an eco-friendly soil stabilization material in sandy environments. *Revista de la Construcción. Journal of Construction*, 23(3), 497-521. <https://doi.org/10.7764/RDLC.23.3.497>

Graphical abstract:



Highlights:

- Biochar significantly impacts shear strength and internal friction angle of sand mixtures.
- Shear strength decreases with biochar up to 10%, then increases with higher content.
- Higher relative density ($D_r=90\%$) shows a greater effect of biochar on mechanical behavior.
- Biochar's influence is stronger at higher normal stress, with friction angle increasing polynomially.

Abstract: This experimental analysis aims to develop a fundamental understanding of the geotechnical properties of soils treated with an organic material named biochar. In this context, an experimental protocol was set using the Casagrande shear box apparatus to effectively demonstrate the combined influence of the biochar fraction ($F_{bio}=0\%$, 5%, 10% and 15%), the initial relative density ($D_r = 20\%$, $D_r = 54\%$, and $D_r = 90\%$), and the initial normal stress ($\sigma_n = 100, 200, \text{ and } 300$

kPa) on the mechanical behavior of Chlef sand. The obtained results clearly show that biochar has a significant influence on the mechanical behavior of the tested materials. Additionally, the shear strength decreases with increasing biochar content up to a threshold value of ($F_{\text{bio}} = 10\%$). Beyond that, the shear strength increases with the increase of biochar content up to the value of ($F_{\text{bio}} = 15\%$) for all the considered parameters. The observed trend of increasing shear strength with the addition of the biochar content ($F_{\text{bio}} = 15\%$) can be attributed to the amplification of the particle interlocking due to the presence of biochar particles between the large particles of Chlef sand, inducing an increase in the dilative character of the tested materials; offering implications for various geotechnical applications. Moreover, pertinent correlations were obtained between the residual shear strength and the grain size characteristics of the sand-biochar mixtures.

Keywords: Chlef sand, biochar, shear strength, interlocking, dilative character.

List of abbreviations

| | |
|---------------------|--------------------------------------|
| C_u | : Coefficient of uniformity |
| C_c | : Coefficient of curvature |
| D_{max} | : Maximum grain size |
| D_r | : Initial relative density |
| e_{max} | : Maximum void ratio |
| e_{min} | : Minimum void ratio |
| e | : Void ratio |
| F_{bio} | : Biochar content |
| G_s | : Specific gravity |
| SP | : Poorly graded sand |
| USCS | : Unified Soil Classification System |
| σ_n | : Normal stress |
| τ | : Shear stress |
| τ_{max} | : Maximum shear stress |
| τ_{res} | : Residual shear stress |
| φ | : Internal friction angle |
| ΔH | : Horizontal displacement |
| ΔV | : Vertical displacement |

1. Introduction

During the last decade, many researches have been focused on the evaluation of new innovative materials to be used in the enhancement of the shear characteristics of granular soils with incorporating the study of its affected parameters (Su and Zhang., 2011; Azaiez et al., 2021a 2021b; Mahmoudi et al., 2020a, 2020b; Latifi et al., 2016; Brahim et al., 2016; Cherif Taiba et al., 2021a,2021b; Phanikumar et al., 2018; Nawagamuwa et al., 2018; Doumi et al., 2021; Taibi et al., 2023a, 2023b; **Wibowo et al 2023**). Indeed, the biochar is an organic material obtained through the thermal degradation of the organic biomass, whereas the activated carbon could be produced from the biomass as well as other carbonaceous substances like a coal (Pardo et al., 2018 and Kazemi et al., 2020). It is typically used in the agricultural and environmental applications and the soils amendment to enhance the physical, chemical and biological characteristics of the granular materials (Pardo et al., 2018).

Moreover, several researchers reported in the published literature, that the production of biochar waste material was related to its inherent characteristics and environmental applications (Figure 1) such as: environmental issues [soil biological properties (Awad et al., 2018; Elazobair et al., 2016) organic contaminants (Dai et al., 2019; Yi et al., 2018; Lyu et al., 2018; Liu et al., 2019)], general characteristics [particle size distribution (Cetin et al., 2004 and Downie et al., 2009, Hazout et al., 2022), mechanical strength (Das et al., 2015; Zickler et al., 2006)], modification techniques [chemical impregnation and properties (Lehmann et al., 2015; Tan et al., 2016; Li et al., 2019; and Agrafioti et al., 2013), microwave modification (Tabalabaei et al., 2019; Yek et al., 2020) and ball milling modification (Cai et al., 2016; Wang et al., 2017).

On the other hand, in the published literature, there are few studies focusing on the influence of biochar content on the mechanical characterization of granular soils. (Lu et al., 2014), performed a series of monotonic direct shear tests on clays mixed with biochar and they confirmed that the addition of biochar increased the shear strength of clays. In addition, they found that the biochar material was at the origin of increasing significantly the internal friction angle of clays. Thus, Mochamad Arief et al., (2015) proved that the biochar had a remarkable effect on the shear strength of sand-biochar mixtures. They also indicated, for a normal stress of 250 kPa and a biochar content of $F_{\text{bio}}=5\%$, the shear strength decreased by 15.3 % compared to pure sand ($F_{\text{bio}}=0\%$), while, biochar percentages of $F_{\text{bio}}=10\%$ and 15% reduced the shear strength by 18.6 % and 22.5 % respectively compared to the shear strength of pure sand ($F_{\text{bio}}=0\%$). Pardo et al., (2018) performed a series of cyclic triaxial tests for the purpose of analyzing the influence of biochar fraction on the mechanical response of the soil. They noticed that increasing the biochar content induced a very significant increase in the cyclic shear strength of the tested soils. Or, the cyclic shear strength of a sand-biochar mixtures for the fraction of ($F_{\text{bio}}=5\%$) was almost six times magnitude compared to the cyclic shear strength of pure sand ($F_{\text{bio}}=0\%$).

Rojimul et al., (2020) conducted a series of triaxial tests on sand mixed with biochar fraction varying from $F_{\text{bio}}=0\%$ to $F_{\text{bio}}=15\%$ for the purpose to investigate the influence of biochar percentage on the shear strength of granular soils. They indicated that biochar content had an important effect on the shear strength of sand-biochar mixtures. They showed that increasing the biochar content from $F_{\text{bio}}=0\%$ to $F_{\text{bio}}=15\%$ induced a remarkable increase in the shear strength of sand-biochar mixtures. Furthermore, they proved that the biochar material had a noticeable impact on the mechanical characteristics in terms of the internal friction angle and cohesion of sand-biochar mixtures (C and ϕ). Rodrigues et al., (2020) found that cyclic shear strength decreased with increasing biochar fraction for the proportion of biochar tested ($F_{\text{bio}}=0\%$, 4% , 5% , and 10%). They reported also that it was very important to note that biochar characteristics depended on its original physical, chemical and mechanical properties in terms of the pyrolysis temperatures and residence times. Sørmo et al. (2024) examined the stabilization of PFAS-contaminated soil using biochar sorbents derived from sewage sludge and wood. Their study evaluated that the application of waste-based biochar sorbents for remediation of contaminated soil can have a positive impact on future waste management practices as this approach leads to a better embodiment of the waste reduction and reuse principles. The main objective of this experimental study is to investigate the impact of biochar fraction ($F_{\text{bio}}=0\%$, 5% , 10% and 15%) on the mechanical behavior of Chlef sand using the direct shear box. Samples of the sand-biochar mixtures were reconstituted in the laboratory with three initial relative densities ($D_r=20\%$, 54% and 90%) and subjected to three normal stresses ($\sigma_n=100\text{ kPa}$, 200 kPa and 300 kPa).

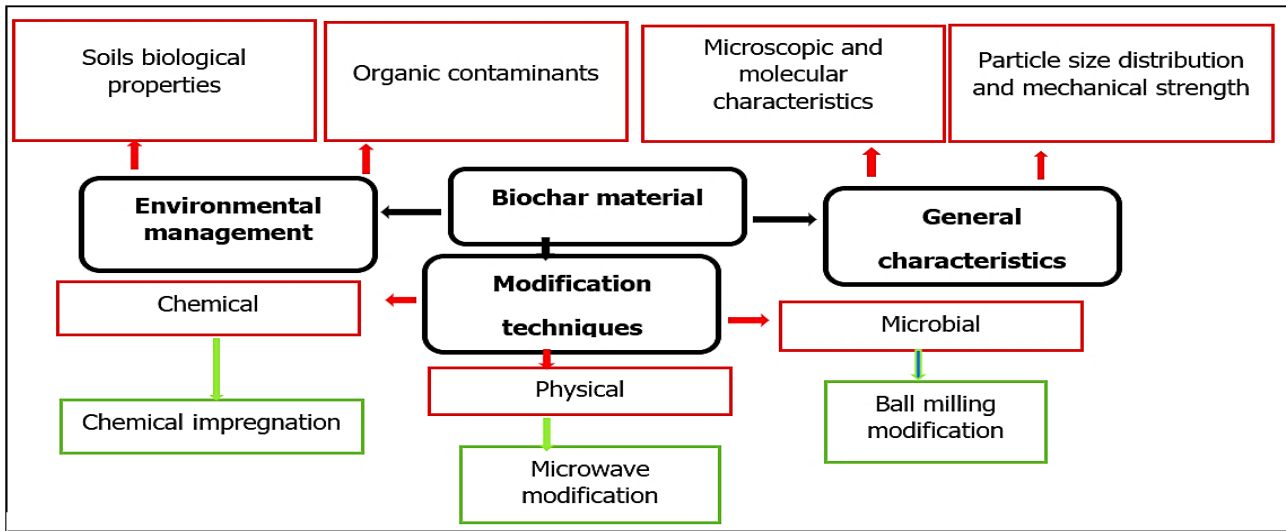


Figure 1. Characteristics and environmental applications of biochar (Kazemi et al., 2020).

2. Index properties of used materials and testing procedure

2.1. Materials

The biochar used in this research was derived from agricultural waste materials sourced from the fertile farmlands of the Mitidja Plain in northern Algeria. Produced through slow pyrolysis at 450°C, this biochar boasts a high carbon content and stable structure. The sandy soil, collected from liquefied soil deposit areas along the banks of the Chlef River in northern Algeria, has a maximum particle diameter of 4.00 mm. This sandy soil was mixed with biochar having a maximum particle diameter of $D_{max}=2.00$ mm, with biochar content varying at 0%, 5%, 10%, and 15%. Both the Chlef sand and biochar have a minimum particle diameter of $D_{min}=0.08$ mm. The chemical composition of the biochar is detailed in Table 1, while the properties of the tested materials are shown in Table 2. The particle size distribution curves of the samples are illustrated in Figure 2 (figure 2a shows the particle size distribution of clean sand and biochar, while, figure 2b presents the particle size distribution of different sand-biochar mixtures). As presented in Figure 3, the void ratios (e_{max} and e_{min}) increase with the addition of biochar (0%, 5%, 10%, and 15%), which can be attributed to the biochar particles filling the spaces between the coarse sand particles, thereby increasing the void ratios in the sand-biochar mixtures.

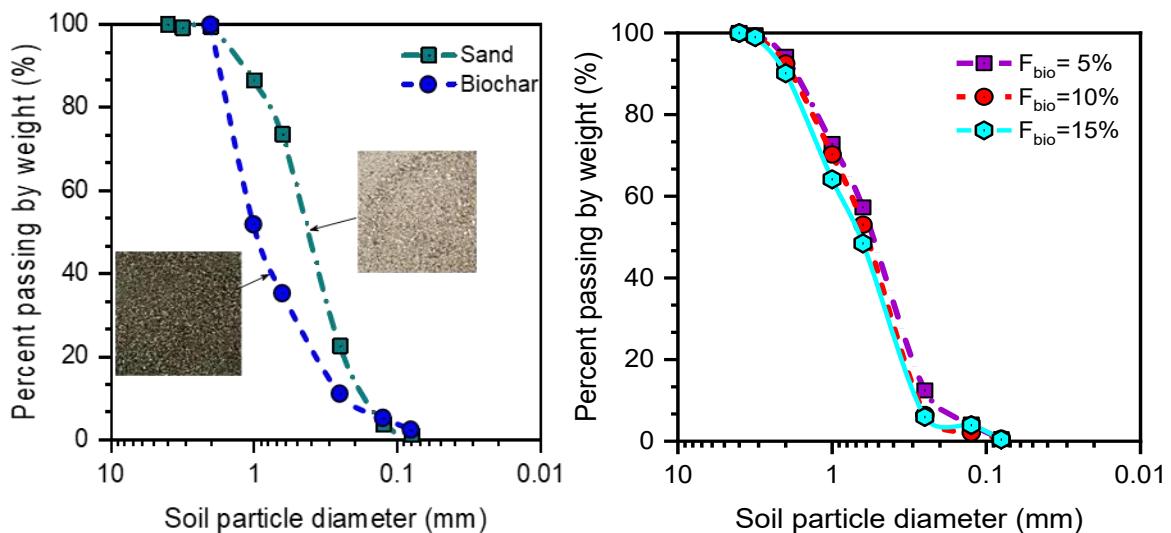


Figure 2. Grain size distribution curves of tested materials: a) clean sand and biochar - b) sand-biochar mixtures.

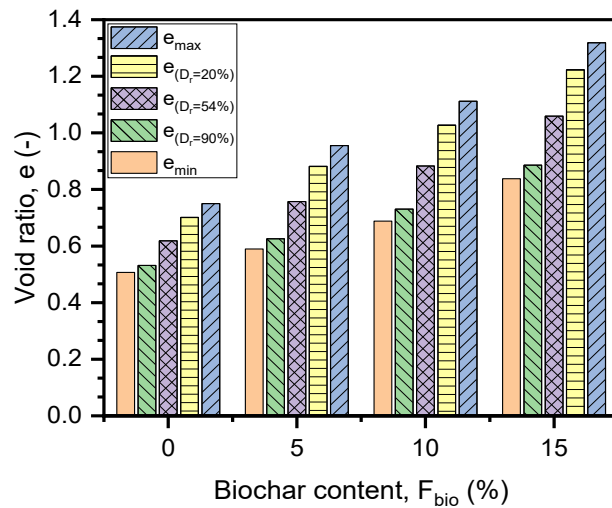


Figure 3. Variation of void ratio as a function of biochar content.

Table 1. Chemical composition of biochar.

| Materials | N | P ₂ O ₅ | K ₂ O | Ca | Mg |
|--------------------------------------|-----|-------------------------------|------------------|--------|-----|
| Content | 0,7 | 0,8 | 3,3 | 4,5 | 0,5 |
| Physico-chemical properties | | | | Valeur | |
| Pyrolysis temperature (°C) | | | | 500 | |
| Pyrolysis time (h) | | | | 5 | |
| Biochar content (%) | | | | 28,26 | |
| PH | | | | 10,28 | |
| Specific surface (m ² /g) | | | | 51,7 | |

Table 2. Physical properties of Chlef sand-biochar mixtures.

| Physical properties | Materials tested | | | | Biochar |
|--|------------------|-------|-------|-------|---------|
| Biochar content, F_{bio} (%) | 0 | 5 | 10 | 15 | 100 |
| Maximum grain size, D_{max} (mm) | 4 | 4 | 4 | 4 | 2 |
| Specific gravity, G_s (-) | 2,66 | 2,57 | 2,481 | 2,391 | 0,88 |
| Effective diameter, D_{10} (mm) | 0,166 | 0,213 | 0,279 | 0,286 | 0,228 |
| Grain size, D_{30} (mm) | 0,229 | 0,305 | 0,442 | 0,465 | 0,548 |
| Mean grain size, D_{50} (mm) | 0,454 | 0,568 | 0,605 | 0,666 | 0,958 |
| Grain size, D_{60} (mm) | 0,529 | 0,695 | 0,779 | 0,902 | 1,169 |
| Coefficient of uniformity, C_u (-) | 3,186 | 3,262 | 2,792 | 3,153 | 5,127 |
| Coefficient of curvature, C_c (-) | 1,059 | 0,628 | 0,898 | 0,838 | 1,126 |
| Maximum global void ratio, e_{max} (-) | 0,75 | 0,955 | 1,112 | 1,319 | 1,755 |
| Minimum global void ratio, e_{min} (-) | 0,507 | 0,589 | 0,688 | 0,838 | 0,866 |

2.2 Testing procedure

A series of direct shear tests was conducted in accordance with NF P94-071-1 (1994) to evaluate the shear properties. The experimental program based on using of one category of sand mixed with biochar contents ($F_{bio} = 0\%$, 5% , 10% and 15%). The sand-biochar sample mixtures were reconstituted by the dry funnel pluviation method with three relative densities ($D_r = 20\%$, 54% and 90%). Thereafter, the tested sand-biochar mixtures were placed in the shear box with size of $60\text{ mm} \times 60\text{ mm} \times 25\text{ mm}$ in depth. A cross section through a typical direct shear device is shown in Figure 4. The soil specimen has a porous stone at the top and bottom to allow free drainage. Above the upper stone is a metal loading cap which is, in turn, subjected to the normal force. The sample and rings are mounted in a tank. The shearing force is applied to the outside of the tank. The samples usually take the form of a square plate, then subjected to three normal stresses ($\sigma_n = 100, 200$ and 300 kPa). All the direct shear tests for this study were conducted at a constant speed (1 mm/min).



Figure 4. Direct shear apparatus.

3. Shearing behaviour of the used soils

3.1. Biochar effects

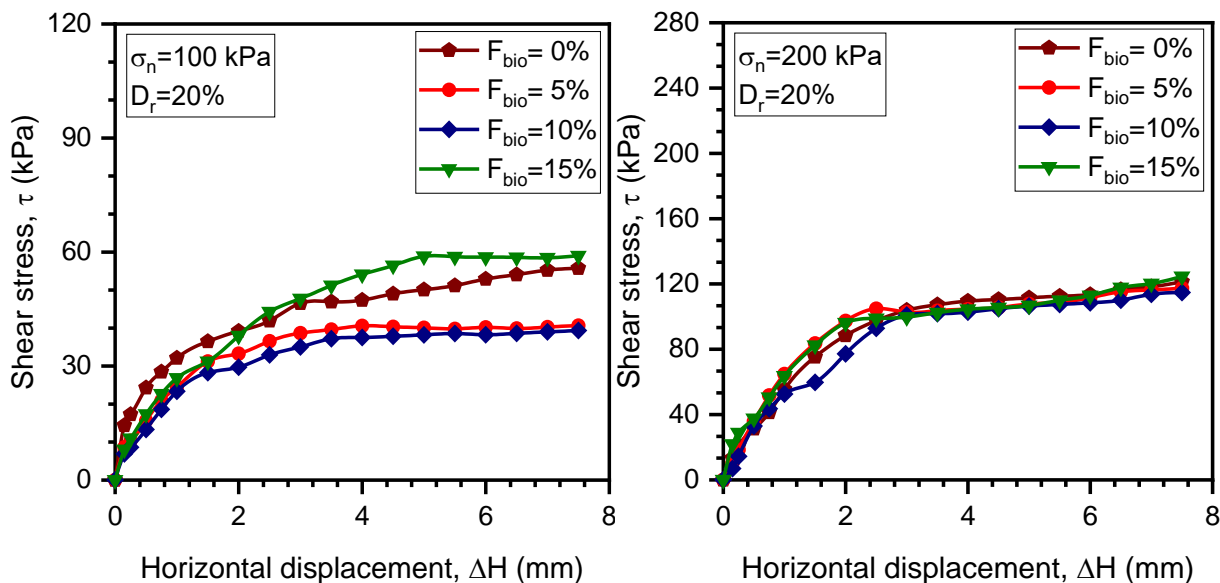
Figures 5, 6 and 7 present the evolution of shear stress versus horizontal displacement of Chlef sand mixed biochar percentages ($F_{bio} = 0\%$, 5% , 10% and 15%). The samples were reconstituted in laboratory with three initial relative densities ($D_r = 20\%$, 54% and 90%) and subjected under three initial normal stresses ($\sigma_n = 100, 200$ and 300 kPa). In general, the obtained results indicate that the biochar parameter has a significant influence on the mechanical response of the sand-biochar mixtures for all parameters studied. Furthermore, the shear strength decreases slightly with increasing of the biochar content up to a threshold of ($F_{bio} = 10\%$). For example, at the normal stress of ($\sigma_n = 100\text{ kPa}$), the residual shear stress decreases from: ($\tau_{max} = 55.75\text{ kPa}$, 40.64 kPa and 39.33 kPa), for relative density ($D_r = 20\%$) considering the three biochar fractions ($F_{bio} = 0\%$, 5% , 10%) respectively.

The shear strength decreasing trend with increasing biochar content up to ($F_{bio} = 10\%$) can be attributed to the biochar grains acting as voids between the sand particles leading to the interlocking decrease of particles and consequently decreasing the resistance of the sand-biochar mixtures. The results of this study are in good agreement with the observations of Rodrigues et al., (2020). On the other hand, beyond this value ($F_{bio} = 10\%$), the shear resistance increases with increasing biochar content ($F_{bio} = 15\%$) for the sand-biochar mixtures studied (Figure 5).

Moreover, the obtained data in Figure (6) confirm that the effect of biochar content on the shearing response is significantly observed for the reconstituted sand-biochar sample mixtures with the medium relative density ($D_r = 54\%$) compared to the loose Chlef sand-biochar mixtures under study. In addition, the test results clearly show that the biochar fraction has a remarkable effect on the mechanical behavior of the sand samples especially in the residual state. However, the impact of biochar fraction on shear strength decreases with increasing biochar content up to a value of $F_{bio} = 10\%$. Where, the sand-biochar mixtures ($F_{bio} = 10\%$) show a decrease in shear strength of (21.68 %, 16.01 %, and 4.21 %) compared to the clean sand samples ($F_{bio} = 0\%$) for the three initial normal stresses ($\sigma_n = 100, 200$ and 300 kPa). On the other hand, the opposite trend is observed for the biochar content ($F_{bio} = 15\%$). Where the shear resistance exhibits an increase of (41.03 %, 12.99 %, and 0.98 %) compared to the specimens of the clean sand ($F_{bio} = 0\%$) for the three initial normal stresses ($\sigma_n = 100, 200$ and 300 kPa) respectively.

In the other hand, Figure 7 presents the variation of shear strength with the horizontal displacement of the dense sand-biochar mixture specimens. It is clearly shown from this Figure that biochar material has a very significant impact on the residual shear state of the dense sand-biochar mixtures ($D_r = 90\%$) compared to the medium dense and loose sand-biochar mixture specimens ($D_r = 54\%$ and 20%). The sand-biochar mixture samples with ($F_{bio} = 10\%$) show a remarkable decrease in shear strength (27.07 % and 1.47 %) for the two initial normal stresses ($\sigma_n = 200$ kPa and 300 kPa), and becomes very pronounced (1.29 %) for the normal stress ($\sigma_n = 100$ kPa) compared to the clean sand specimens ($F_{bio} = 0\%$) (Figure 7a, b, c).

However, the sand-biochar mixtures with ($F_{bio} = 15\%$) indicate a notable increase in shear strength (9.6 % and 32.14 %) for the two initial normal stresses ($\sigma_n = 200$ kPa and 300 kPa), and becomes very pronounced (5.94 %) for the normal stress ($\sigma_n = 100$ kPa) in comparison to the clean sand specimens ($F_{bio} = 0\%$) under consideration (Figure 7a, b, c). In addition, Figures 8, 9, and 10 present the evolution of vertical displacement as a function of horizontal displacement, taking into account the influence of biochar content. In general, the vertical displacement results obtained confirm the shear resistance results, where, the addition of the biochar fraction decreases the dilation phase/increases the contractive behaviour up to a certain biochar threshold of $F_{bio} = 10\%$. However, beyond this threshold, an inverse trend was observed, where the biochar fraction ($F_{bio} = 15\%$) leads to a decrease in the contractive character/increase in the dilative character compared to the threshold content ($F_{bio} = 10\%$), which then translates into an increase in the shear strength of this mixture.



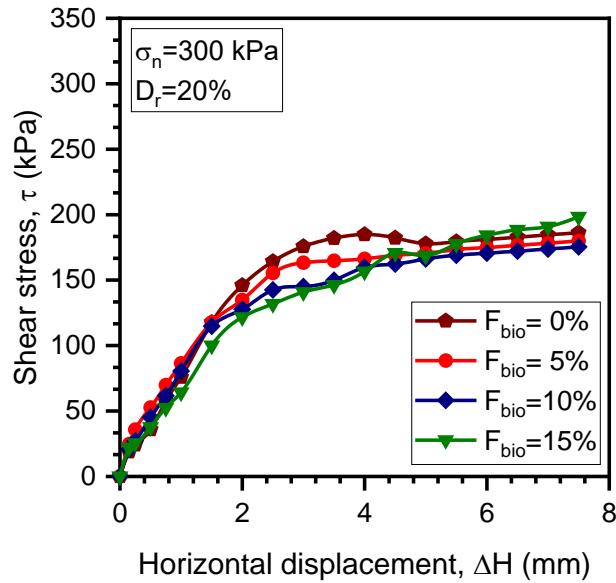
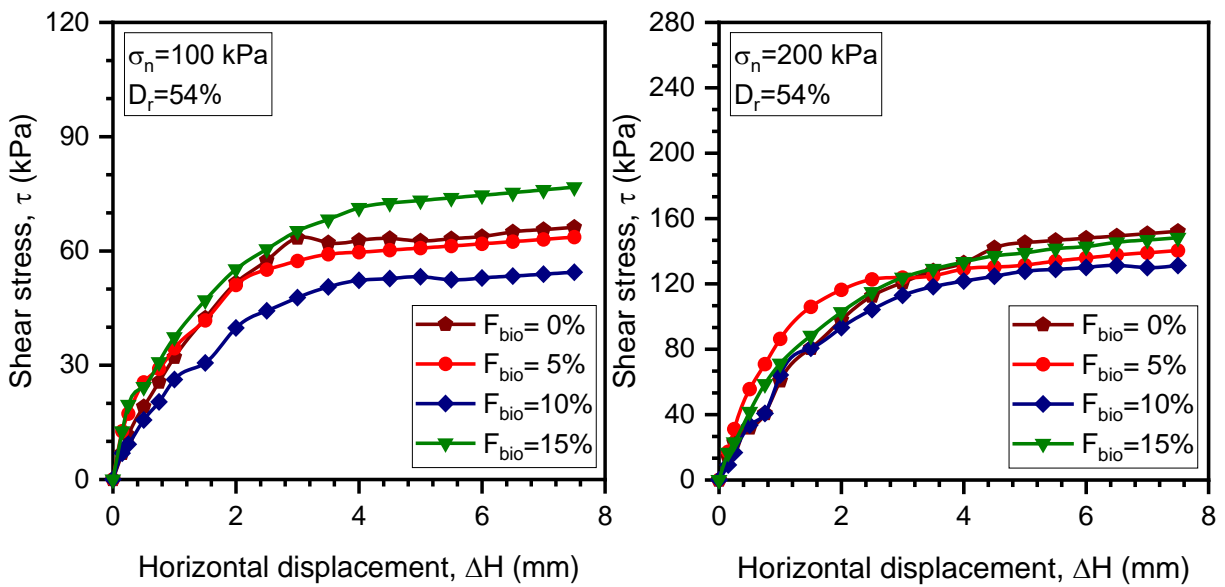


Figure 5. Mechanical behavior of sand-biochar mixtures ($D_r=20\%$)
(a)- $\sigma_n=100$ kPa, (b)- $\sigma_n=200$ kPa, (c)- $\sigma_n=300$ kPa.



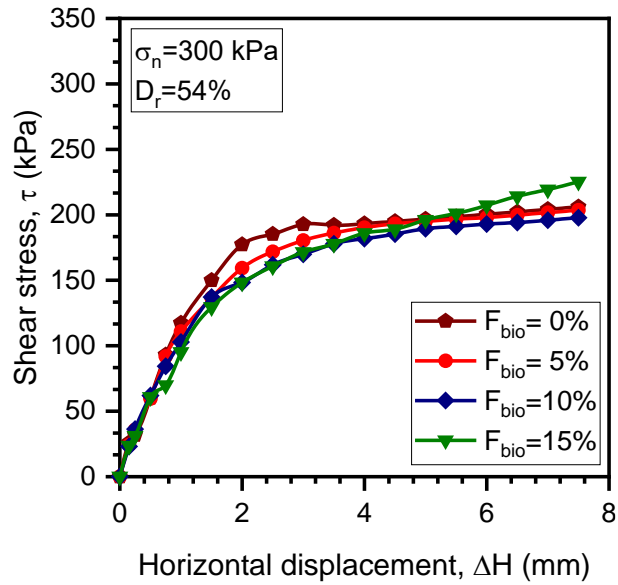
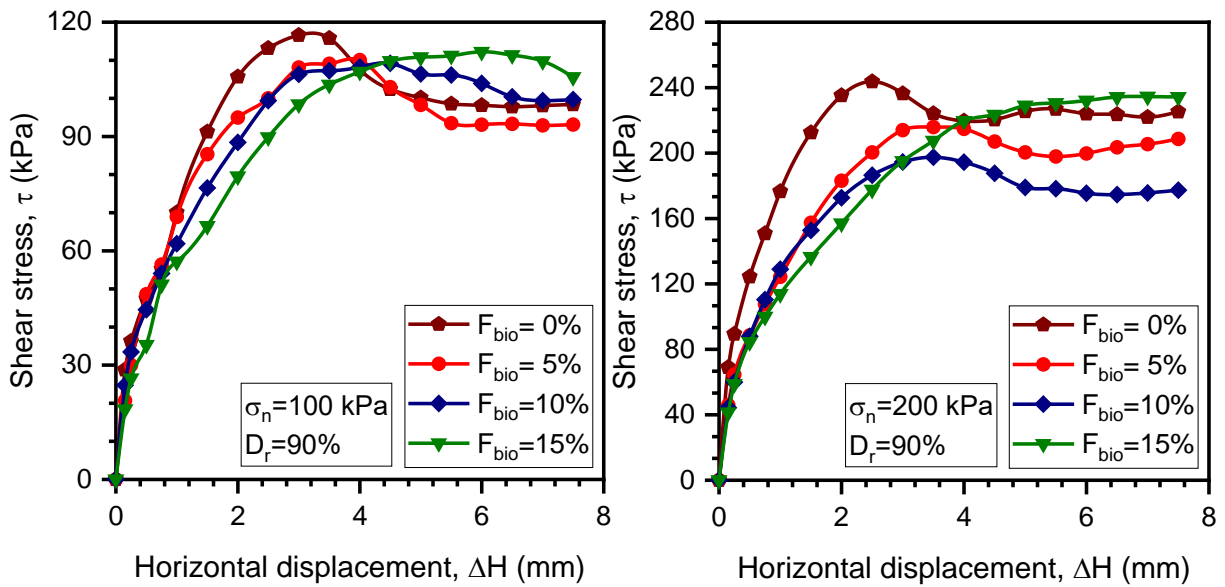


Figure 6. Mechanical behavior of sand-biochar mixtures ($D_r=54\%$)
(a)- $\sigma_n=100$ kPa, (b)- $\sigma_n=200$ kPa, (c)- $\sigma_n=300$ kPa.



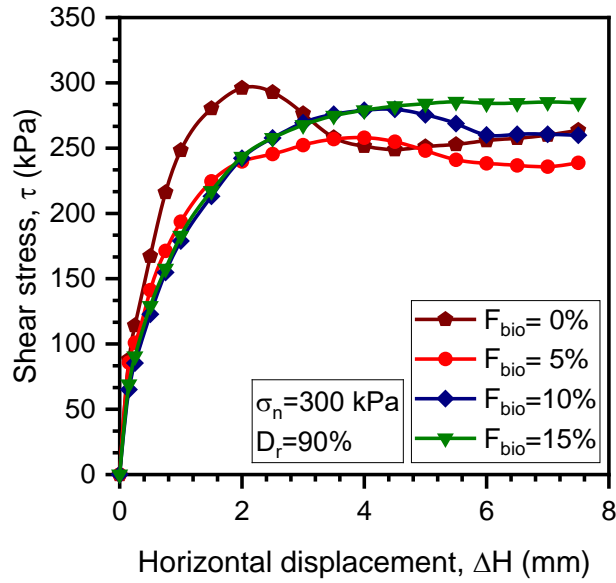
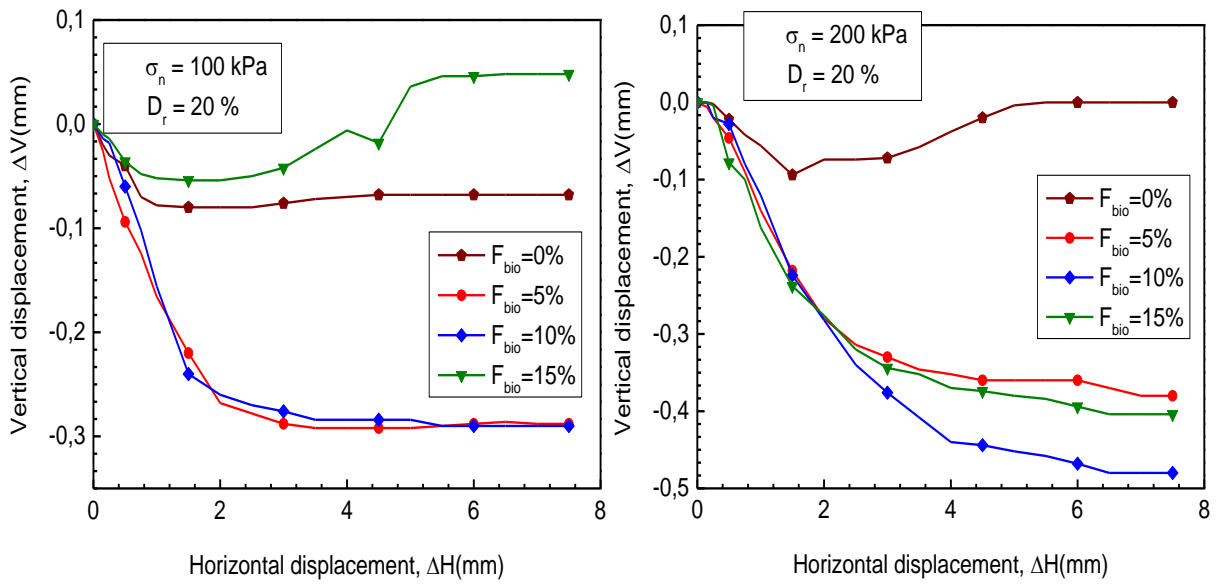


Figure 7. Mechanical behavior of sand-biochar mixtures ($D_r=90\%$).
(a)- $\sigma_n=100$ kPa, (b)- $\sigma_n=200$ kPa, (c)- $\sigma_n=300$ kPa.



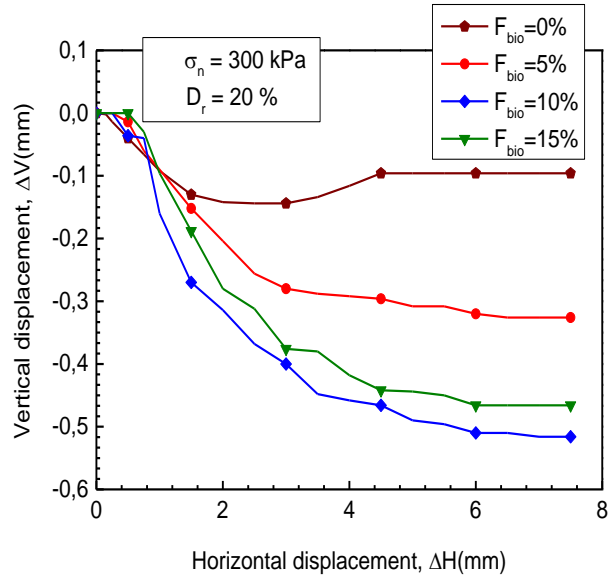
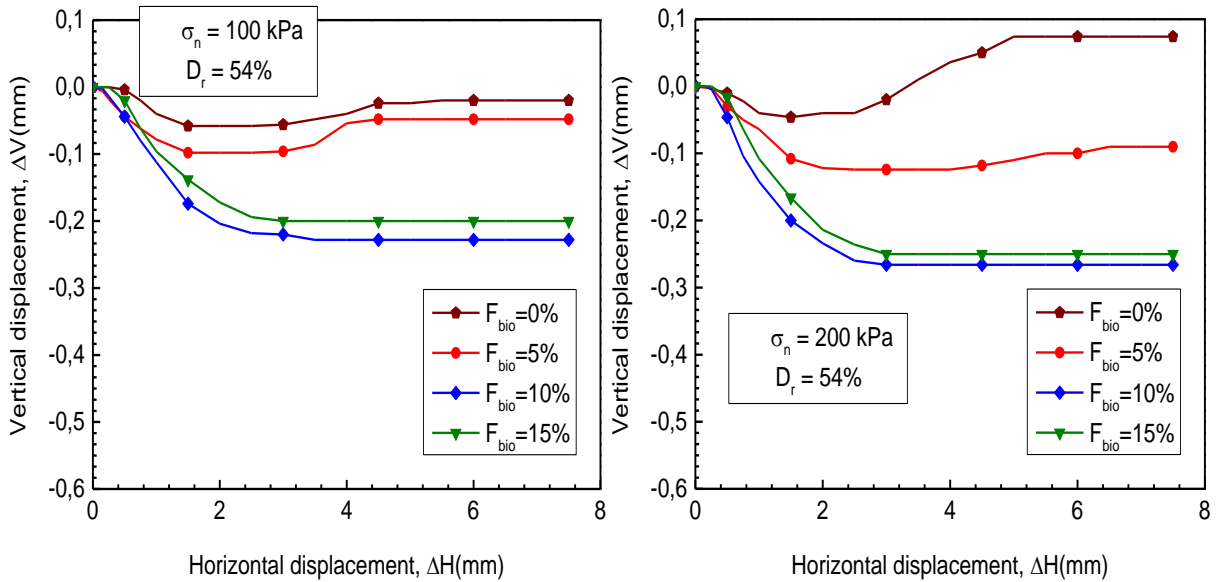


Figure 8. Vertical displacement versus horizontal displacement ($D_r=20\%$)
(a)- $\sigma_n=100$ kPa, (b)- $\sigma_n=200$ kPa, (c)- $\sigma_n=300$ kPa.



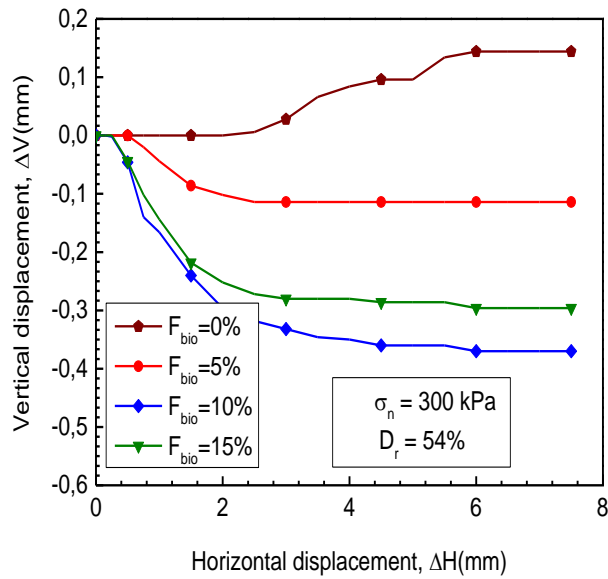
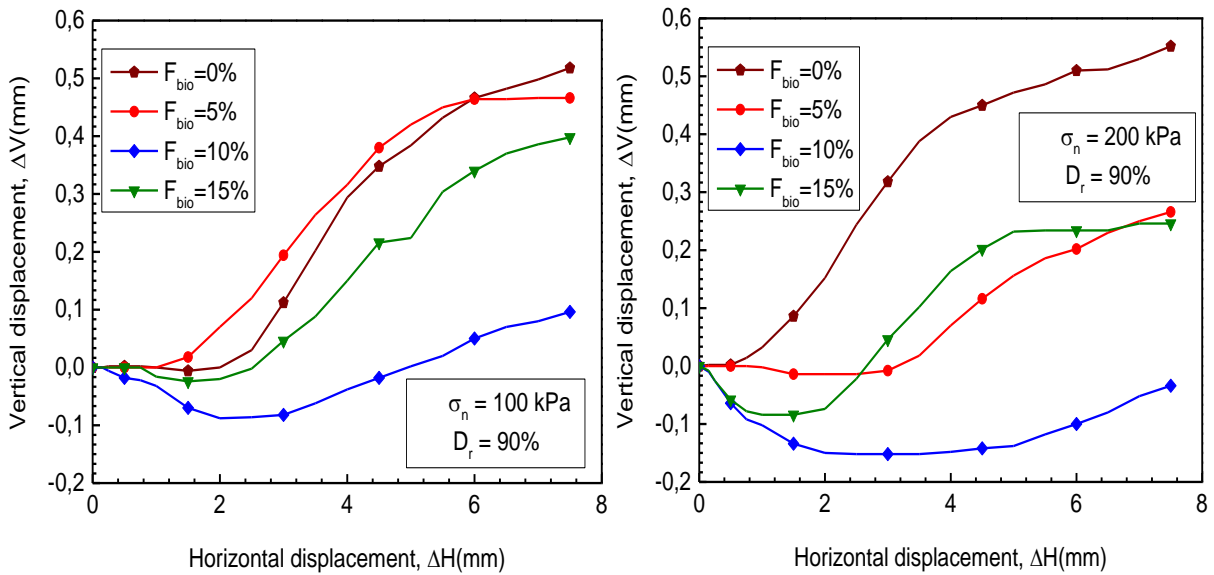


Figure 9. Vertical displacement versus horizontal displacement ($D_r=54\%$)
(a)- $\sigma_n = 100$ kPa, (b)- $\sigma_n = 200$ kPa, (c)- $\sigma_n = 300$ kPa.



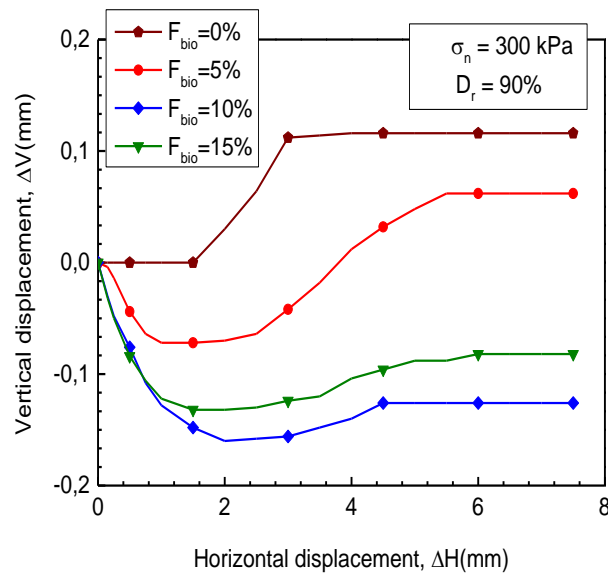


Figure 10. Vertical displacement versus horizontal displacement ($D_r=90\%$)
(a)- $\sigma_n=100$ kPa, (b)- $\sigma_n=200$ kPa, (c)- $\sigma_n=300$ kPa.

3.2. Relative density effects

A series of direct shear tests were conducted to investigate the influence of initial relative density (loose; $D_r=20\%$, medium dense; $D_r=54\%$, and dense; $D_r=90\%$) on the mechanical behavior of sand-biochar mixtures, Figures (11, 12 and 13) are established. The sand-biochar mixtures were reconstructed in the laboratory with the dry funnel pluviation method, subjected under three initial normal stresses ($\sigma_n = 100$ kPa, 200 kPa and 300 kPa) and mixed with four biochar contents ($F_{bio} = 0\%$, 5%, 10% and 15%). The obtained test results clearly show that the relative density parameter has a very relevant impact on the shear strength of sand-biochar mixtures. For example, at the biochar content of ($F_{bio}=0\%$), the residual shear stress increases from: ($\tau_{res}=55.75$ kPa, 66.22 kPa and 98.38 kPa) considering the three initial relative densities ($D_r=20\%$, 54% and 90%), respectively, as shown in Figures (11a). The effect of initial relative density on the increase in shear strength is clearly observed for the range of relative density ($D_r=20\% - 54\%$) (15.81%, 36.12%, 27.73%, and 18.82%) and becomes very significant for the range of relative density ($D_r=54\% - 90\%$) (48.56%, 46.35%, 83.14%, and 37.61%) for the considered biochar fractions ($F_{bio}=0\%$, 5%, 10%, and 15%) respectively. This increase in shear strength is due to the role of relative density which increases the interlocking of the mixtures which promotes a more dilative behavior leading to an increase in shear strength with a more stable sample structure.

In addition, Figure (12) presents the evolution of shear strength with the horizontal displacement of the sand-biochar mixtures subjected under a normal stress ($\sigma_n = 200$ kPa). As can be seen from this figure that increasing in the initial relative density induces a significant increase in the shear strength of sand-biochar mixtures. This increase in shear strength remains insignificant (20.26%, 16.35%, 12.52% and 18.14%) for the range of relative density ($D_r=20\% - 54\%$) and becomes very pronounced (48.04%, 48.66%, 35.13% and 58.04%) for the range of relative density ($D_r=54\% - 90\%$) considering the different biochar fractions ($F_{bio}=0\%$, 5%, 10% and 15%) respectively. Moreover, the residual shear strength of sand-biochar mixtures subjected to an initial normal stress ($\sigma_n = 200$ kPa) shows high values ($\tau_{res} = 117.4$ kPa, 140.35 kPa and 208.65 kPa) for ($F_{bio}=5\%$) (Figure 12b) in comparison to the maximum shear strength values for the sand-biochar mixtures tested under initial normal stress ($\sigma_n = 100$ kPa) (Figure 11b). In the other hand, the sand-biochar mixtures reconstituted with the relative density $D_r = 90\%$ indicate a very significant increasing in maximum shear strength of (41.61%, 32.75%, 48.18%, and 47.84%) for the biochar fractions ($F_{bio}=0\%$, 5%, 10%, and 15%), respectively, compared to the specimens reconstituted with the loose relative density ($D_r = 20\%$). Furthermore, the obtained results clearly indicate that the specimens of the sand-biochar mixtures subjected to an initial normal stress ($\sigma_n = 300$ kPa) indicate higher residual shear strengths ($\tau_{res} = 175.36$ kPa, 197.75

kPa, and 259.85 kPa) for ($F_{bio}=10\%$) (Figure 13c) compared to the sand-biochar mixtures tested under the other two normal stresses ($\sigma_n = 100$ kPa and 200 kPa) (Figure 11c and Figure 12c).

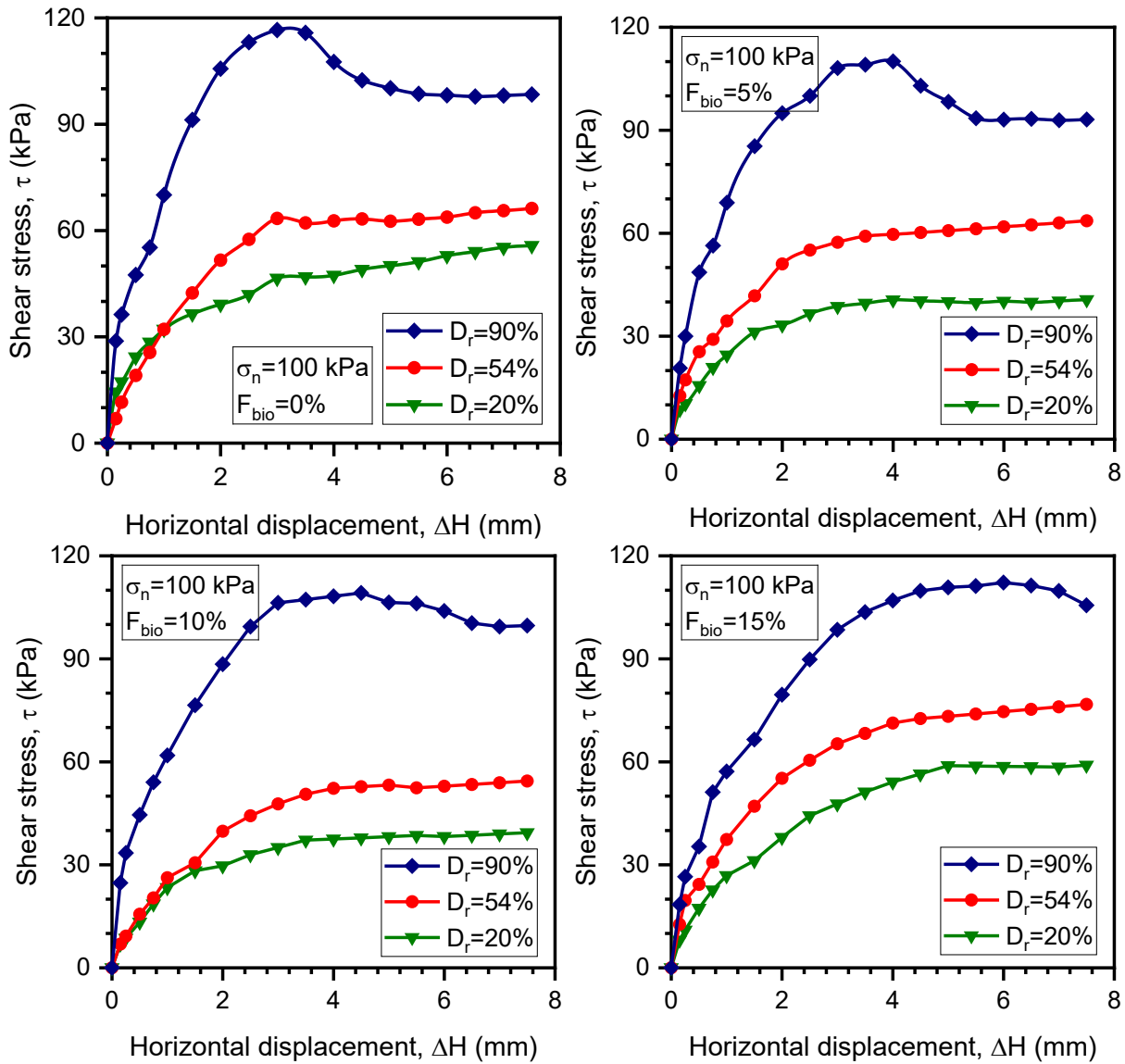


Figure 11. Effect of initial relative density on the mechanical behavior of the sand-biochar mixtures ($\sigma_n=100$ kPa) (a)- $F_{bio}=0\%$, (b)- $F_{bio}=5\%$, (c)- $F_{bio}=10\%$, (d)- $F_{bio}=15\%$.

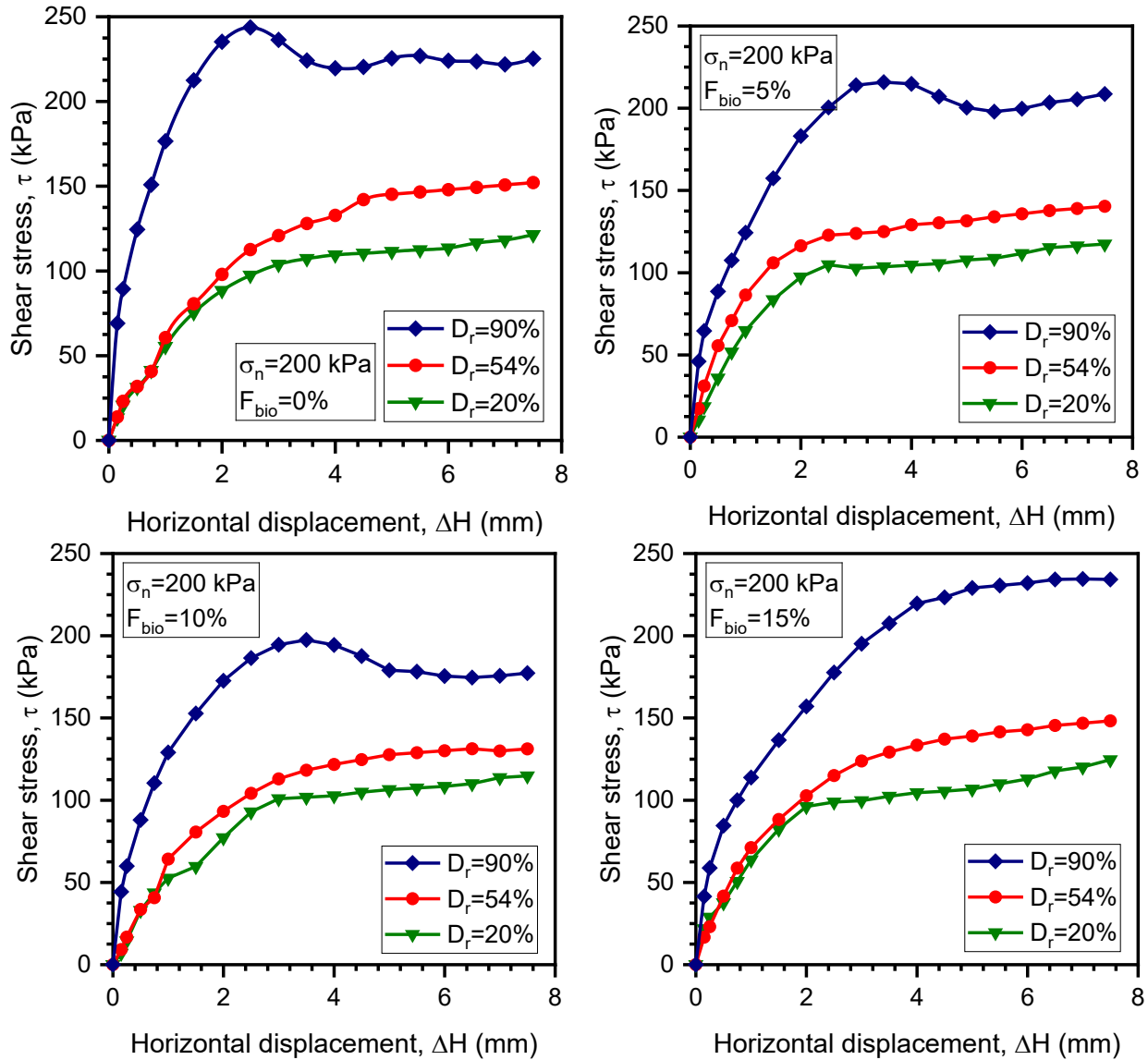


Figure 12. Effect of initial relative density on the mechanical behavior of the sand-biochar mixtures ($\sigma_n=200$ kPa)
(a)- $F_{bio}=0\%$, (b)- $F_{bio}=5\%$, (c)- $F_{bio}=10\%$, (d)- $F_{bio}=15\%$.

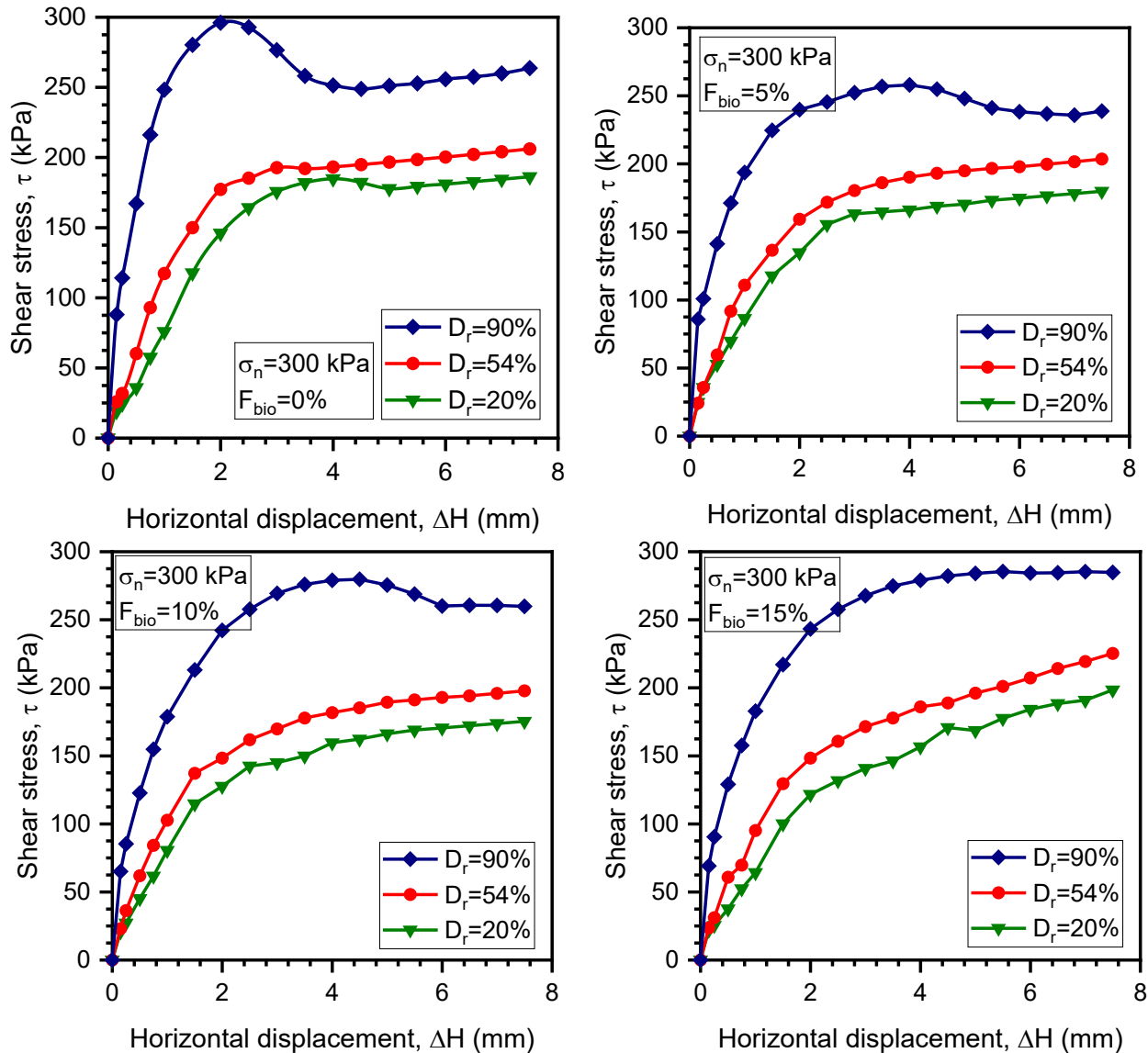


Figure 13. Effect of initial relative density on the mechanical behavior of the sand-biochar mixtures ($\sigma_n=300$ kPa) (a)- $F_{bio}=0\%$, (b)- $F_{bio}=5\%$, (c)- $F_{bio}=10\%$, (d)- $F_{bio}=15\%$.

4. Residual shear stress of the sand-biochar mixtures

Figure (14) shows the evaluation of the influence of the biochar proportions on the residual shear stress of Chlef sand for a range of biochar content varying from $F_{bio}=0\%$ to $F_{bio}=15\%$. The mixtures were reconstituted in laboratory with three initial relative densities ($D_r=20\%$, 54% and 90%) considering three initial normal stresses ($\sigma_n = 100, 200$ and 300 kPa). From this figure, it can be seen that the parameter of biochar content is a very relevant parameter in the study of the mechanical response of sandy soils, where the residual shear stress decreases with increasing of the biochar fraction ($0\% \leq F_{bio} \leq 10\%$) for the three initial relative densities and three initial normal stresses under consideration. In contrast, an inverse trend is observed in the range of ($10\% \leq F_{bio} \leq 15\%$), where the residual shear stress increases with increasing biochar fraction for all parameters studied. Furthermore, the residual shear stress decreases with increasing of the biochar fractions ($0\% \leq F_{bio} \leq 10\%$) for the loose and the medium relative densities ($D_r=20\%$, 54%) and becomes very pronounced for the higher relative density ($D_r=90\%$). In contrast, for the biochar content ranges ($10\% \leq F_{bio} \leq 15\%$), the residual shear stress increases with increasing biochar fractions and it more significant for the dense sand-biochar mixture specimens ($D_r=90\%$) compared to the sand-biochar

mixture specimens reconstituted with ($D_r=20\%$ and 54%) respectively. Furthermore, the influence of biochar fraction is very remarkable for the higher initial normal stress ($\sigma_n = 300\text{ kPa}$) compared to the other two initial normal stresses ($\sigma_n = 100$ and 200 kPa) for all tested parameters under study.

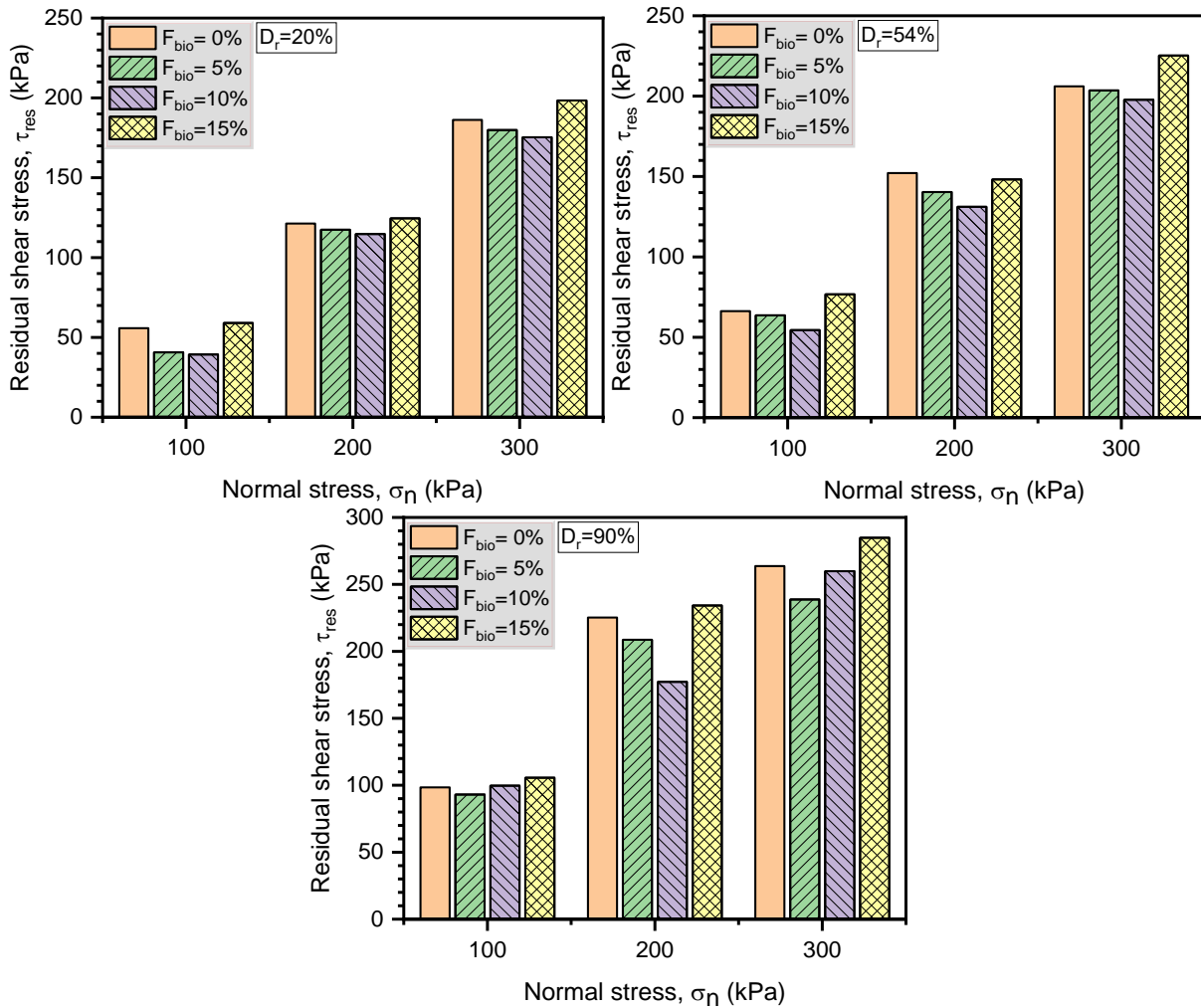


Figure 14. Residual shear stress versus normal stress of the sand-biochar mixtures.

5. Combined effects of relative density and normal on residual shear stress of the sand-biochar mixtures

The combined effects of the relative density (D_r) and normal stress (σ_n) on the residual shear stress (τ_{res}) of Chlef sand mixed with four percentages of biochar materials ($F_{bio} = 0\%$, 5% , 10% and 15%) are illustrated in Figure 15. As it can be seen, the obtained results indicate that the relative density and the normal stress have a considerable effect on the residual shear stress of the used sand-biochar mixtures. In addition, it clearly seen from the 3D plot that there exists a good correlation between (τ_{res}) with (D_r) and (σ_n) for the binary mixtures. Indeed, the residual shear stress increases in linear manner with the increase of the relative density from ($D_r=20\%$ to $D_r=90\%$) and the normal stress from ($\sigma_n=100\text{ kPa}$ to 300 kPa) for all tested materials under study. This behaviour confirms that the amplification of the relative density and the normal stress lead increase the inter-particle forces between the coarse grains of sand and biochar particles and consequently conducting to a significant increasing of the residual shear stress of the sand-biochar mixture specimens. Moreover, the correlation between the residual shear stress with the relative density and the normal stress is more relevant for the sand-biochar mixtures with ($F_{bio} = 15\%$) compared to other biochar content ($F_{bio} = 0\%$, 5% and 10%) for all the studied parameter under consideration (Figure 15).

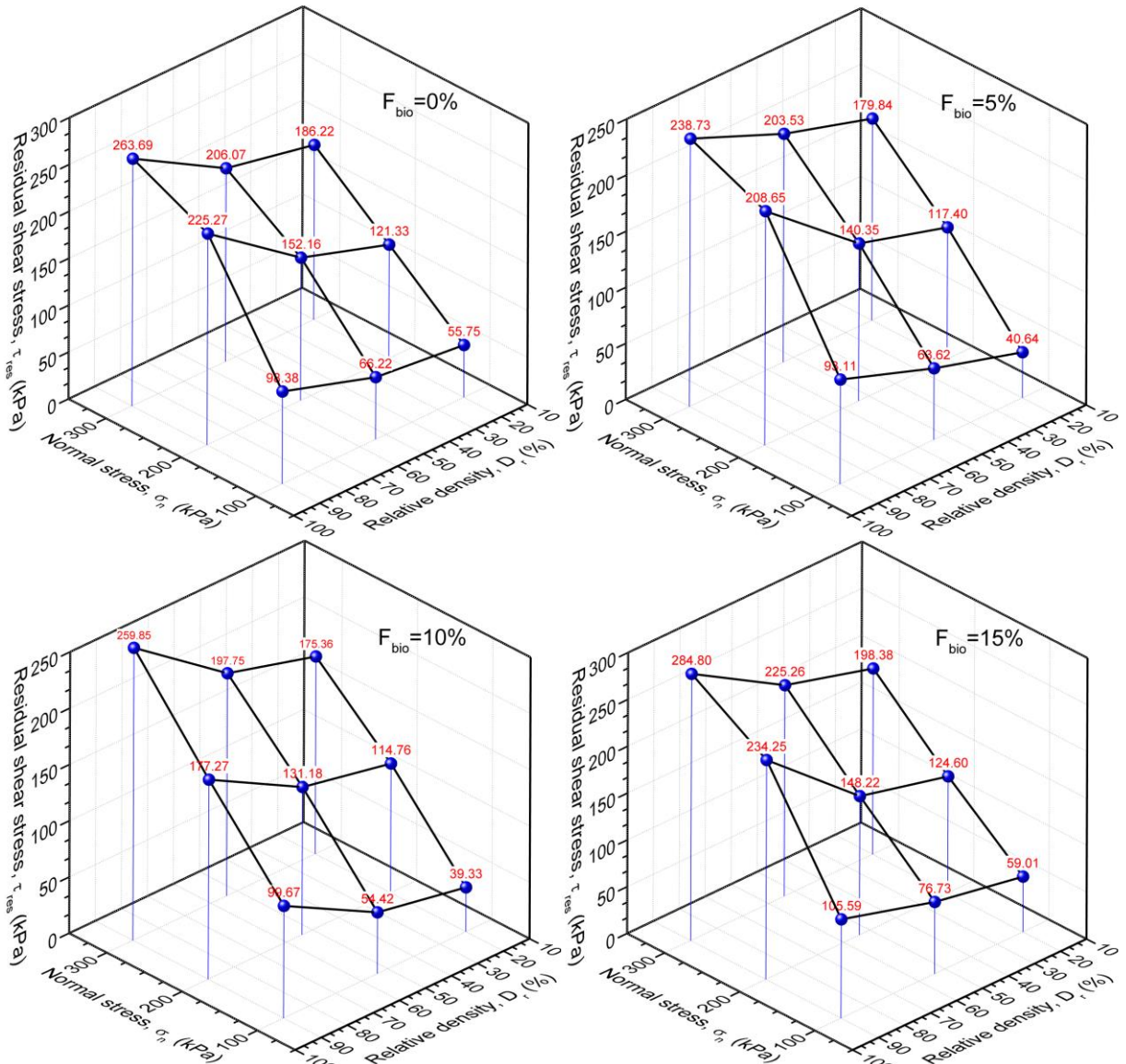


Figure 15. Residual shear stress versus normal stress and relative density of the sand-biochar mixtures.

6. Correlation between residual shear stress with grain size characteristics and biochar content of the tested materials

The impacts of grain size (D_{30} , D_{60}), effective diameter (D_{10}), mean diameter (D_{50}) and coefficient of uniformity (C_u) on the residual shear stress of the tested sand-biochar mixture samples for the biochar content ranging from ($F_{bio}=0\%$ to $F_{bio}=15\%$), relative densities ($D_r=20\%$ and 90%) and normal stresses ($\sigma_n=100$ kPa and 300 kPa) are presented in this section. It can be observed from Figures (16, 17, 18 and 19) that, a linear relationship may express between residual shear stress with grain diameters and biochar content of the tested binary mixtures under consideration. In addition, the residual shear stress decreases with the decrease of grain size properties until the biochar content ($F_{bio}=10\%$). Beyond this value, the residual shear stress increases with the decrease of the particle sizes characteristics (D_{10} , D_{30} , D_{50} and D_{60}) of the reconstituted materials at two initial relative densities ($D_r=20\%$ and 90%) and tested under two initial normal stresses ($\sigma_n=100$ kPa and 300 kPa) under study. However, Figure (20) illustrates the correlation between residual shear stress, coefficient of uniformity (C_u), and biochar content of sand-biochar mixtures. The plots reveal no consistent correlation between residual shear stress and coefficient

of uniformity (C_u) across the all range of biochar contents examined. Where, for biochar contents ranging from 0% to 5%, residual shear stress decreases as the coefficient of uniformity increases. Beyond that, it continues to decrease with the increase of C_u until ($F_{bio}=10\%$) for the loose density samples, while, the dense samples exhibit an opposite trend in this range. Interestingly, for biochar contents between 10% and 15%, the relationship shifts. At 15% biochar content, the residual shear stress increases with the increase of uniformity coefficient. The obtained data confirm that the biochar content plays a major role in changing of the particle size characteristics of the mixtures and consequently affect the mechanical behaviour of the tested binary assemblies under study.

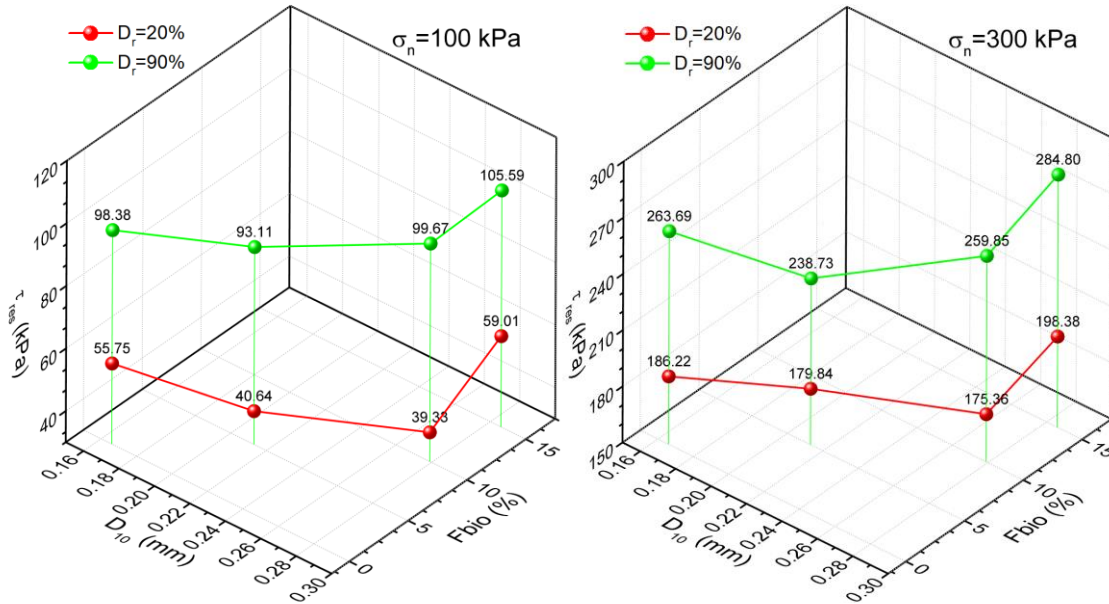


Figure 16. Residual shear stress versus effective diameter (D_{10}) and biochar content of the sand-biochar mixtures.

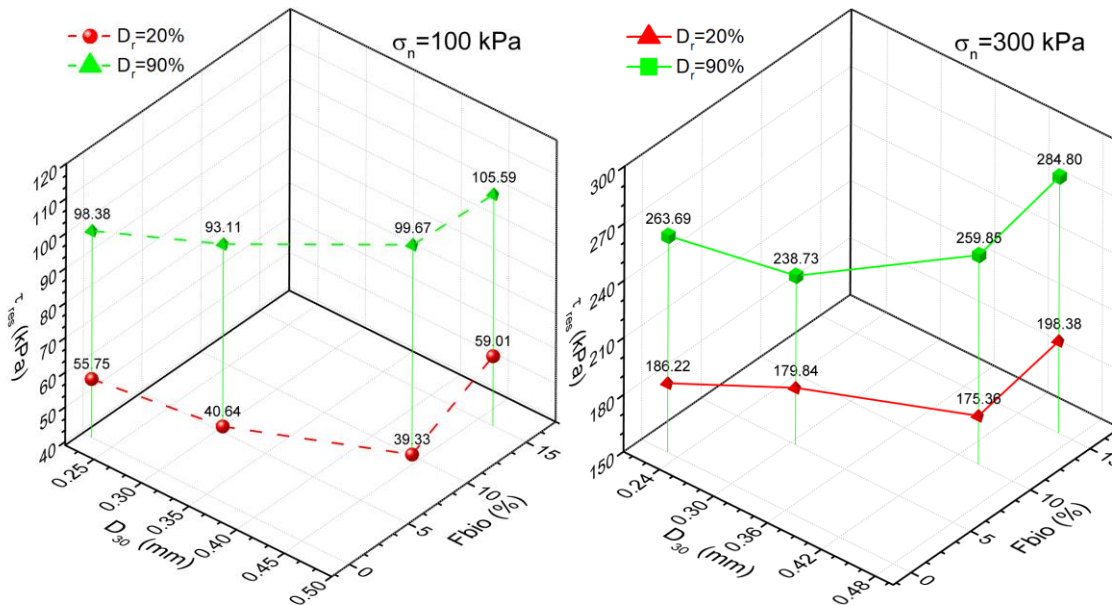


Figure 17. Residual shear stress versus Grain size (D_{30}) and biochar content of the sand-biochar mixtures.

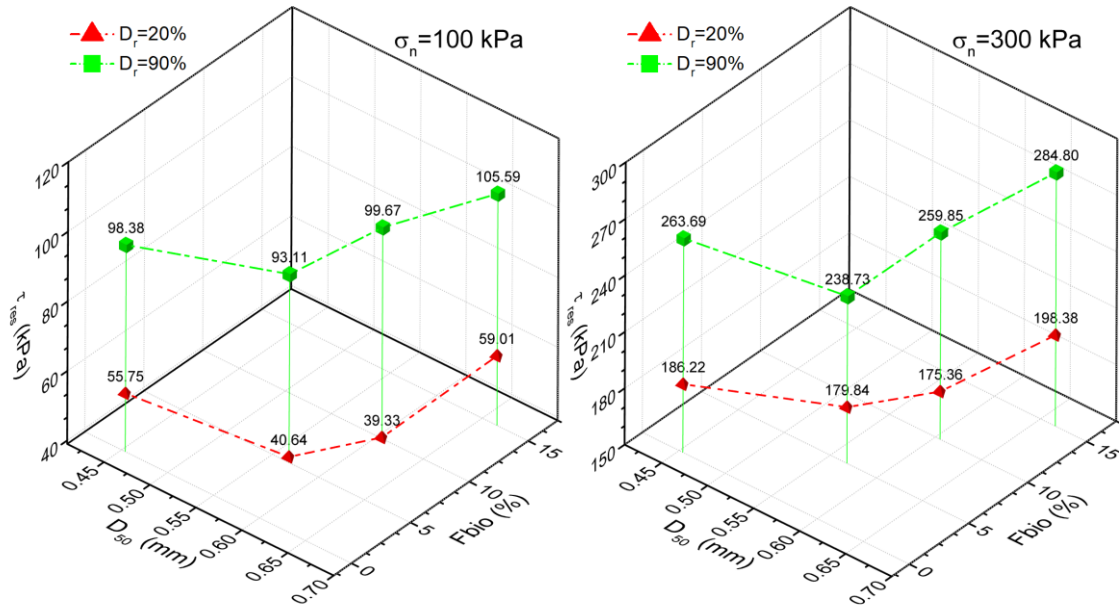


Figure 18. Residual shear stress versus mean diameter (D_{50}) and biochar content of the sand-biochar mixtures.

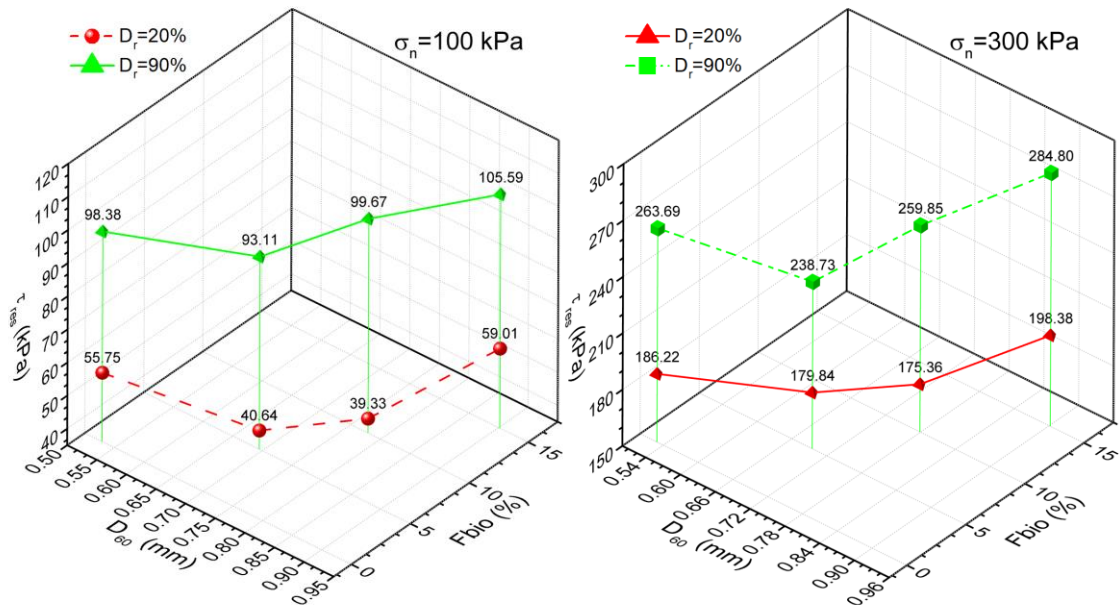


Figure 19. Residual shear stress versus Grain size (D_{60}) and biochar content of the sand-biochar mixtures.

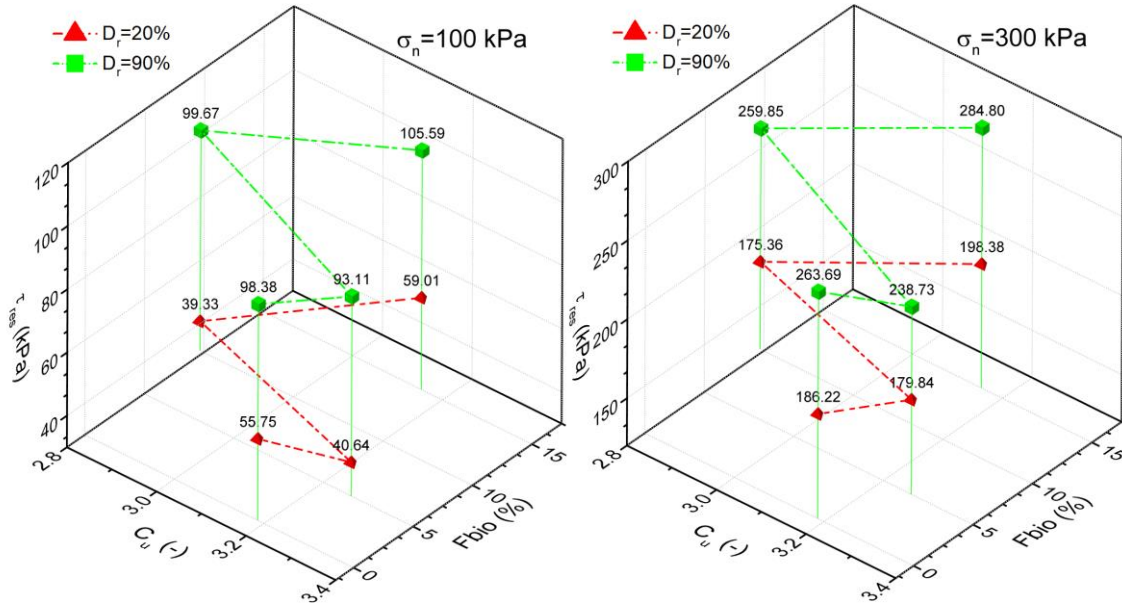


Figure 20. Residual shear stress versus coefficient of uniformity and biochar content of the sand-biochar mixtures.

7. Correlation between the internal friction angle with biochar content and relative density of the tested materials

For the purpose of analyzing the correlation between the internal friction angle (φ) with the biochar content (F_{bio}) and relative density (D_r) of the reconstituted samples with three different relative densities (20 %, 54 % and 90 %) and the range of biochar percentages (0 %, 5 %, 10 % and 15 %), Figure 21 illustrates the test results obtained from the current study. In general, it could be noticed from this Figure, the existence of relevant polynomial relationships between the angle of internal friction and the relative density for the sand-biochar mixtures considering the four biochar fractions under study. Indeed, the internal friction angle increases with the increase of the relative density for all the tested binary assemblies. Moreover, the obtained results indicate very good correlations between the internal friction angle and the initial relative density ($R^2=0.99$) for all biochar fractions studied. In other hand, it is clearly shown from this Figure that the sand-biochar mixtures ($F_{bio}=15\%$) exhibit higher values of the internal friction angles compared to the other biochar content ($F_{bio}=0\%$, 5% and 10%) for all the tested initial relative densities ($D_r=20\%$, 54% and 90%) respectively. The following equation is suggested to express the evolution of the internal friction angle (φ) as a function of the relative density for the sand-biochar mixtures under consideration.

$$(\varphi) = a \times (D_r)^2 + b \times (D_r) + c \quad (1)$$

Table 3. Coefficients a, b et R^2 pour l'équation (1).

| F_{bio} (%) | 0 | 5 | 10 | 15 |
|---------------|---------|---------|---------|---------|
| a | 0.0018 | 0.0004 | 0.0006 | 0.0015 |
| b | -0.1351 | -0.0256 | -0.0058 | -0.0658 |
| R^2 | 0.99 | 0.99 | 0.99 | 0.99 |

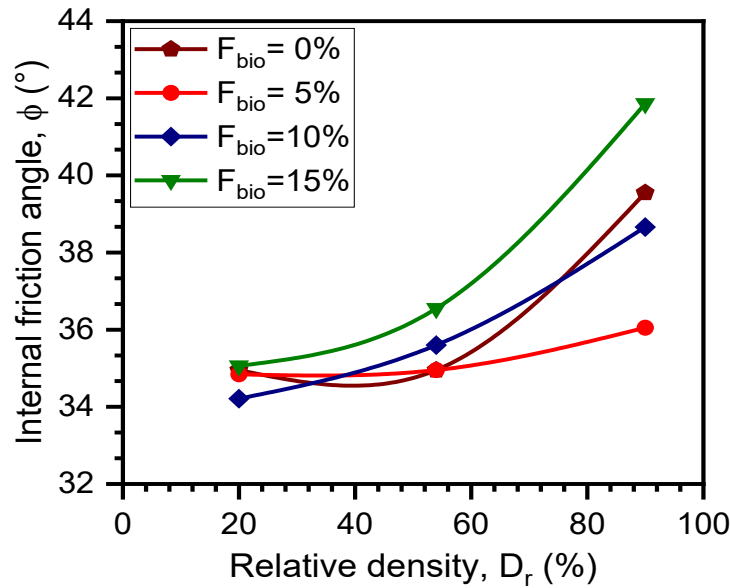


Figure 21. Internal friction angle versus relative density for the sand-biochar mixtures.

8. Potential of woody biochar: eco-friendly soil stabilization for sustainable environmental technology

The integration of woody biochar in sandy soils not only holds promise for environmental sustainability but also bears significant implications for soil mechanics, particularly in the context of direct shear testing on sand-biochar mixtures. The addition of biochar alters the mechanical behavior of sandy soils, influencing parameters such as shear strength, stiffness, and deformation characteristics. Direct shear testing provides invaluable insights into the shear behavior of these mixtures under varying conditions, shedding light on their stability and load-bearing capacity. By subjecting sand-biochar mixtures to direct shear tests, researchers can discern the effects of biochar content, particle size, and compaction on shear strength parameters such as cohesion and internal friction angle. Understanding these mechanical properties is crucial for engineering applications ranging from slope stability assessments to foundation design in construction projects. Furthermore, insights gained from direct shear testing can inform the optimal utilization of woody biochar in soil stabilization efforts, ensuring both environmental benefits and structural integrity.

Thus, the relationship between woody biochar and direct shear testing underscores the interdisciplinary nature of addressing environmental challenges while advancing soil mechanics and engineering practices. On the other hand, the potential implementation of woody biochar in the stabilization of sandy soils represents a significant stride in environmental technology. Sandy soils are notoriously prone to erosion and nutrient leaching, leading to decreased fertility and compromised ecosystem health. By introducing woody biochar—a carbon-rich material derived from biomass pyrolysis—we not only enhance soil structure and water retention but also sequester carbon, mitigating greenhouse gas emissions. This eco-friendly approach addresses the dual challenges of soil degradation and climate change. Moreover, woody biochar serves as a sustainable alternative to conventional soil stabilizers, reducing reliance on synthetic chemicals and promoting natural soil processes. Through the integration of woody biochar into soil management practices, we harness the power of nature to foster resilient ecosystems while advancing environmental sustainability.

9. Conclusion

The performed experimental investigation aims to study the influence of the biochar content ($F_{bio}=0\%$, 5% , 10% and 15%) on the geotechnical properties of Chlef sandy soils reconstituted in the laboratory with three initial relative densities ($D_r=20\%$, $D_r=54\%$ and $D_r=90\%$) using the dry funnel pluviation method and subjected to three initial normal stresses ($\sigma_n=100$, 200 and 300 kPa). Based on the obtained experimental results, the following conclusions can be drawn:

1. The results of the direct shear box tests clearly show that the biochar material has a remarkable influence on the mechanical behavior of sand-biochar mixtures in terms of the maximum shear strength and the internal friction angle.
2. The shear strength decreases with increasing the biochar content up to a value of $F_{bio}=10\%$, the results of this study are in perfect agreement with the observations of Rodrigues et al., (2020). Beyond this value, the shear strength increases with increment of the biochar content up to the value of $F_{bio}=15\%$ for the tested parameters. This tendency may be explained by the fact that the addition of higher amounts of biochar play a major role in increasing the inter-particle forces between the sand and consequently increasing the geotechnical properties of the materials under study.
3. The results of the different tests indicate clearly that the addition of biochar content has a remarkable influence on the mechanical behavior of the sand-biochar mixtures for the higher initial relative density ($D_r=90\%$) compared to the other two initial relative densities ($D_r=20\%$, $D_r=54\%$).
4. The test results indicate that the impact of biochar content is highly significant for the highest initial normal stress ($\sigma_n=300$ kPa) compared to the other two normal stresses ($\sigma_n=100$ and 200 kPa). Furthermore, the obtained results indicate that the friction angle increases in a polynomial manner with increasing the relative density for all tested parameters. The obtained data confirm that the particle size characteristics (D_{10} , D_{30} , D_{50} and D_{60}) have pertinent influences on the shear response of the sand-biochar binary assemblies compared to the coefficient of uniformity (C_u).
5. On the other hand, the application of the biochar material in the civil engineering field, especially, for geotechnical engineering purposes is still in the preliminary stages, and its suitability is under evaluation and the future researches should take care to its implementation in the geotechnical engineering field. Studying the properties of the biochar and its effects on the geotechnical characterization of granular materials is highly recommended in the future studies.

Acknowledgments: The authors are thankful to all those who effectively contributed to the achievement of this laboratory investigation.

Data Availability Statement: All data, models, and code generated or used during the study appear in the submitted article.

Compliance with ethical standards

Conflicts of interest: The authors declare that they have no conflict of interest.

References

- Agrafioti, E., Bouras, G., Kalderis, D., and Diamadopoulos, E. (2013). Biochar production by sewage sludge pyrolysis. *Journal of analytical and applied pyrolysis*, 101, 72-78.
- Awad, Y. M., Ok, Y. S., Abrigata, J., Beiyuan, J., Beckers, F., Tsang, D. C., and Rinklebe, J. (2018). Pine sawdust biomass and biochars at different pyrolysis temperatures change soil redox processes. *Science of the Total Environment*, 625, 147-154.
- Azaiez, H., Taiba, A. C., Mahmoudi, Y., and Belkhatir, M. (2021). Characterization of granular materials treated with fly ash for road infrastructure applications. *Transportation Infrastructure Geotechnology*, 8, 228-253.
- Azaiez, H., Cherif Taiba, A., Mahmoudi, Y., and Belkhatir, M. (2021). Shear characteristics of fly ash improved sand as an embankment material for road infrastructure purpose. *Innovative Infrastructure Solutions*, 6(3), 148.
- Abdelkader, B., Ahmed, A., Mostéfa, B., and Isam, S. (2016). Laboratory study of geotextiles performance on reinforced sandy soil. *Journal of Earth Science*, 27(6), 1060-1070.
- Abdelkader, B., Arab, A., Sadek, M., and Shahrour, I. (2018). Laboratory investigation of the influence of geotextile on the stress-strain and volumetric change behavior of sand. *Geotechnical and Geological Engineering*, 36(4), 2077-2085.
- Cai, H., Xu, L., Chen, G., Peng, C., Ke, F., Liu, Z., ... and Wan, X. (2016). Removal of fluoride from drinking water using modified ultrafine tea powder processed using a ball-mill. *Applied Surface Science*, 375, 74-84.
- Cherif Taiba, A., Mahmoudi, Y., Belkhatir, M., and Baille, W. (2021). Assessment of the correlation between grain angularity parameter and friction index of sand containing low plastic fines. *Geomechanics and Geoengineering*, 16(2), 133-149.
- Cherif Taiba, A., Mahmoudi, Y., Belkhatir, T., Witchmann, M., Baille, W. (2021b). Threshold Silt Content Dependency on Particle Morphology (Shape and Size) of Granular Materials: Review with New Evidence. *Acta geotechnica Slovenica* 18 (1): 28-40. DOI: 10.18690/actageotechslv.18.1.28-40.2021

- Cherif Taiba, A., Mahmoudi, Y. and Belkhatir, M. (2024). Discussion of "Experimental Study on Unconfined Compressive Strength of Rubberized Cemented Soil" by Jie He, Duanwei Guo, Dexin Song, Fangcheng Liu, Lei Zhang, and Qifeng Wen. *KSCE J Civ Eng*. <https://doi.org/10.1007/s12205-024-1998-z>
- Cetin, E., Moghtaderi, B., Gupta, R., and Wall, T. F. (2004). Influence of pyrolysis conditions on the structure and gasification reactivity of biomass chars. *Fuel*, 83(16), 2139-2150.
- Dai, Y., Zhang, N., Xing, C., Cui, Q., and Sun, Q. (2019). The adsorption, regeneration and engineering applications of biochar for removal organic pollutants: a review. *Chemosphere*, 223, 12-27.
- Das, O., Sarmah, A. K., and Bhattacharyya, D. (2015). Structure–mechanics property relationship of waste derived biochars. *Science of the Total Environment*, 538, 611-620.
- Doumi, K., Mahmoudi, Y., Cherif Taiba, A., Baille, W., and Belkhatir, M. (2021). Influence of the particle size on the flow potential and friction index of partially saturated sandy soils. *Transportation Infrastructure Geotechnology*, 1-25.
- Downie, A., Crosky, A., Munroe, P., (2009). Physical properties of biochar. In: Lehmann, J., Joseph, S. (Eds.), *Biochar for Environmental Management: Science and Technology*, 1th ed. Earthscan Publication Ltd., London, UK; Sterling, VA, USA, pp. 13-32.
- Elzobair, K.A., Stromberger, M.E., Ippolito, J.A., Lentz, R.D., (2016). Contrasting effects of biochar versus manure on soil microbial communities and enzyme activities in an Aridisol. *Chemosphere* 142, 145-152.
- Hazout, L., Cherif Taiba, A., Mahmoudi, Y., and Belkhatir, M. (2022). Deformation characteristics of natural river sand under compression loading incorporating extreme particle diameters impacts. *Marine Georesources and Geotechnology*, <https://doi.org/10.1080/1064119X.2022.2122090>.
- Kazemi, H.S.P, Dehghani, M, Yong S.O, Nizami, A.S, Khoshnevisan, B, Solange I. M, Aghbashlo, M, Tabatabaei, M, Su S. L. (2020). A comprehensive review of engineered biochar: Production, characteristics, and environmental applications. *Journal of Cleaner Production* 270.122462. doi.org/10.1016/j.jclepro.2020.122462
- Latifi, N., A. S. A. Rashid, S. Siddiqua, and M. Z. A. Majid. (2016). "Strength measurement and textural characteristics of tropical residual soil stabilised with liquid polymer." *Measurement* 91: 46–54. <https://doi.org/10.1016/j.measurement.2016.05.029>
- Lehmann, J., Joseph, S., (2015). *Biochar for Environmental Management: Science, Technology and Implementation*. Routledge.
- Li, H., Lu, X., Xu, Y., and Liu, H. (2019). How close is artificial biochar aging to natural biochar aging in fields? A meta-analysis. *Geoderma*, 352, 96-103.
- Liu, J, Wang, Y, Kanungo, D. P, Wei, J, Bai, Y., Li, D, Lu, Y. (2019). Study on the Brittleness Characteristics of Sand Reinforced with Polypropylene Fiber and Polyurethane Organic Polymer. *Fibers and Polymers*, 20(3), 620-632. DOI :10.1007/s12221-019-8779-1
- Lu, W., Ding, W., Zhang, J., Li, Y., Luo, J., Bolan, N., Xie, Z., (2014). Biochar suppressed the decomposition of organic carbon in a cultivated sandy loam soil: a negative priming effect. *Soil Biol. Biochem.* 76, 12-21.
- Lyu, H., Gao, B., He, F., Zimmerman, A.R., Ding, C., Huang, H., Tang, J., (2018). Effects of ball milling on the physicochemical and sorptive properties of biochar: experimental observations and governing mechanisms. *Environ. Pollut.* 233, 54-63.
- Mahmoudi, Y., Cherif Taiba, A., Hazout, L. Belkhatir, M., and Baille, W. (2020a). Packing Density and Overconsolidation Ratio Effects on the Mechanical Response of Granular Soils. *Geotechnical and Geological Engineering journal*, DOI 10.1007/s10706- 019-01061-2
- Mahmoudi, Y. Cherif Taiba, A. Belkhatir, M. Baille, W and Wichtmann, T. (2020b). Characterization of mechanical behavior of binary granular assemblies through the equivalent void ratio and equivalent state parameter. *European Journal of Environmental and Civil Engineering*. 24 (8) DOI.org/10.1080/19648189.2020.1775708
- Mochamad A. B, A. Chegenizadehb, H., Nikrazc (2015). Investigation of the strength of carbon-sand mixture. *Procedia Engineering* 102 (2015) 634-639, Doi: 10.1016/j.proeng.2015.01.153.
- Nawagamuwa, U. P., and Wijesooriya, N. (2018). Use of fly ash to improve soil properties of drinking water treatment sludge. *International Journal of Geo-Engineering*, 9, 1-8.
- NF P94-071-1 (1994). *Sols : reconnaissance et essais - Essai de cisaillement rectiligne à la boîte - Partie 1 : cisaillement direct*. AFNOR.
- Pardo, G. S., Orense, R. P., and Sarmah, A. K. (2018). Cyclic strength of sand mixed with biochar: Some preliminary results. *Soils and foundations*, 58(1), 241-247.
- Phanikumar, B. R., and Nagaraju, T. V. (2018). Effect of fly ash and rice husk ash on index and engineering properties of expansive clays. *Geotechnical and Geological engineering*, 36(6), 3425-3436.
- Rodrigues De Amorim, R., Orense, R. P., Pardo, G. S., Sarmah, A. K., and Yan, W. M. (2020). Liquefaction resistance of sand amended with biochar. *Géotechnique Letters*, 10(2), 290-295.
- Hussain, R., Ghosh, K. K., Garg, A., and Ravi, K. (2021). Effect of biochar produced from mesquite on the compaction characteristics and shear strength of a clayey sand. *Geotechnical and Geological Engineering*, 39, 1117-1131.

- Su, T., and X. C. Zhang. (2011). Effects of EN-1 soil stabilizer on slope runoff hydraulic characteristics of Pisha sandstone stabilized soil. *Trans. Chin. Soc. Agric. Mach.* 42 (11): 68–75.
- Sørmo, E., Lade, C. B. M., Zhang, J., Asimakopoulos, A. G., Åsli, G. W., Hubert, M., ... & Cornelissen, G. (2024). Stabilization of PFAS-contaminated soil with sewage sludge-and wood-based biochar sorbents. *Science of the Total Environment*, 922, 170971.
- Tabatabaei, M., Aghbashlo, M., Dehghani, M., Kazemi Shariat Panahi, H., Mollahosseini, A., Hosseini, M., (2019). Reactor technologies for biodiesel production and processing: a review. *Prog. Energy Combust. Sci.* 74, 239-303.
- Taibi, A., Mahmoudi, Y., Cherif Taiba, A., Azaiez, H., and Belkhatir, M. (2023). Fly ash effects on the stress-dilatancy relation of coarse soils: Particle morphology role. *Geotechnical and Geological Engineering*, 41(4), 2517-2536.
- Taibi, A., Mahmoudi, Y., Taiba, A. C., Azaiez, H., and Belkhatir, M. (2023). Influence of particle size index on shear properties of cohesionless soils admixture with fly ash binder. *Journal of Geo Engineering*, 18(2).
- Tan, X.-f., Liu, Y.-g., Gu, Y.-l., Xu, Y., Zeng, G.-m., Hu, X.-j., Liu, S.-b., Wang, X., Liu, S.-m., Li, J., (2016). Biochar-based nano-composites for the decontamination of wastewater: a review. *Bioresour. Technol.* 212, 318-333.
- Wang, B., Gao, B., Fang, J., (2017). Recent advances in engineered biochar productions and applications. *Crit. Rev. Environ. Sci. Technol.* 47, 2158-2207.
- Wibowo, Dian Eksana, Ramadhan, Dymas Agung, Endaryanta, & Prayuda, Hakas. (2023). Soil stabilization using rice husk ash and cement for pavement subgrade materials. *Revista de la construcción*, 22(1), 192-202. <https://dx.doi.org/10.7764/rdlc.22.1.192>.
- Yek, P.N.Y., Peng, W., Wong, C.C., Liew, R.K., Ho, Y.L., Mahari, W.A.W., Azwar, E., Yuan, T.Q., Tabatabaei, M., Aghbashlo, M., (2020). Engineered biochar via microwave CO₂ and steam pyrolysis to treat carcinogenic Congo Red Dye. *J. Hazard Mater.* 122636.
- Yi, S., Sun, Y., Hu, X., Xu, H., Gao, B., Wu, J., (2018). Porous nano-cerium oxide wood chip biochar composites for aqueous levofloxacin removal and sorption mechanism insights. *Environ. Sci. Pollut. Res.* 25, 25629-25637.
- Zickler, G., Schoberl, T., Paris, O., (2006). Mechanical properties of pyrolysed wood: a nanoindentation study. *Philos. Mag. A* 86, 1373-1386.
- Alhazmi, T., and McCaffer, R. (2000). Project procurement system selection model. *Journal of Construction Engineering and Management*, 126(3), 176-184.



Copyright (c) 2024. Megrouse, M., Mahmoudi, Y., Cherif Taiba, A., Azaiez, H. and Belkhatir, M. This work is licensed under a [Creative Commons Attribution-NonCommercial-No Derivatives 4.0 International License](https://creativecommons.org/licenses/by-nc-nd/4.0/).